Rapid Characterization of Geosynchronous Space Debris with 5-color Near-IR Photometry

Dr. Eric C. Pearce
Steward Observatory, University of Arizona

Dr. H. Alyson Ford
Steward Observatory, University of Arizona

Dr. Thomas Schildknecht
Astronomical Institute, University of Bern

Dr. Vishnu Reddy
Lunar and Planetary Laboratory, University of Arizona

Adam D. Block
Steward Observatory, University of Arizona

Kris Rockowitz
Steward Observatory, University of Arizona

ABSTRACT

The characterization of deep space debris has posed a significant challenge in SSA. To be most operationally effective, characterization must be performed quickly and under non-ideal operational conditions, generally using non-resolved techniques. The use of multi-color photometry and the resultant color indices in the near and short-wave IR offer the potential to rapidly discriminate between debris and intact space objects such as rocket bodies and satellites. Specifically, the color indices surrounding the near-IR Z band (0.83-0.925 μm) show promise to differentiate materials while providing a more practical data collection opportunity when compared to spectroscopy. Similar techniques have been demonstrated in the astronomical community to discriminate between different classes of near Earth asteroids. The diagnostic attributes of the Z band are particularly compelling as similar diagnostic color indices can be measured using visible telescopes and the corresponding Sloan z' band. Initial results of an extensive survey of cataloged debris, high area-to-mass ratio (HAMR) objects, rocket bodies, and intact satellites with the UK IR Telescope (UKIRT) Wide Field Camera (WFCAM) are presented to assess the efficacy of these techniques. As a test case, an ensemble of Russian SL-12 rocket bodies (SL-12 RB) discarded in geosynchronous orbit has been studied. Using the techniques described above, one of these rocket bodies (2012-012D, SCN 38104) has been identified having anomalous near-IR spectral characteristics compared to all others in the study. Additionally, this object experiences unusual secular perturbations in its post-mission orbital elements.

1. INTRODUCTION

Since the launch of Sputnik in 1957, space surveillance has tracked and studied satellites and space debris with optical telescopes. The first attempts to use optical photometry to characterize satellites were published by the U.S and Russians in the late 1950s [1, 2]. The excellent historical review papers by Lambert [3] and Sukhov [4] summarize much of the history of photometric technique development in the US and Russia respectively. The US Ground Based Electro-Optical Space Surveillance (GEODSS) system would rely on the themes originally presented by Moore in [1] to assess the stability and spin rate of deep space satellites by analysis of the broadband reflected

brightness of the satellite as it spun or changed illumination geometry [5]. Although not adopted in the original GEODSS system, Souvari suggests in [5] that multi-color photometry could be used to distinguish satellite materials, and notes the criticality of multi-color measurements being made simultaneously to remove the effects of other variations in the brightness of satellites with time such as rotation and phase angle changes. M. Payne would extensively study the efficacy of multi-color photometry for satellite characterization using a filter set specifically optimized for SSA [6, 7]. Additionally, multi-color Johnson-Cousins VRI photometry and light curve observations of high AMR objects were acquired with AIUB's 1 meter ZIMLAT telescope [8].

Characterizing satellites by color indices offers several advantages that are important to SSA: (a) the color indices are less dependent on variable atmosphere extinction and thus more robust in poor observing conditions, (b) multi-color photometric instrumentation is relatively simple and inexpensive, and (c) due to the lower spectral resolution, higher signal-to-noise measurements can be collected with smaller telescopes and less observing time than that required for higher resolution spectroscopic measurements.

Most satellite photometric techniques developed for SSA since the initial deployment of the GEODSS system have focused on extracting detailed material properties or even "inverting" the photometric signature to reveal a shape model. In contrast to these approaches, we endeavor to develop techniques that can be rapidly applied to newly discovered objects to identify unusual or non-historic objects and allow cueing for more detailed study. One example of a relevant operational scenario at GEO (geosynchronous Earth orbit) is to identify solar-panel covered microsatellites from neighboring space debris after an on-orbit event. The authors have demonstrated a method of satellite characterization using multi-color near-IR photometry, using primarily color indices in the Z, Y, and J bands using the UK IR Telescope (UKIRT) Wide Field Camera (WFCAM). Reference [9] outlines the capabilities of UKIRT to track and measure satellites and space debris with the WFCAM and [10] describes the WFCAM instrument itself.

This paper describes the initial results of approximately 250 h of survey time with the WFCAM, most of which was focused on characterizing space debris and rocket bodies. Observational techniques that are adaptable to our goal of rapidly characterizing space objects were developed and refined. These techniques have been applied to an ensemble of Russian SL-12 rocket bodies (SL-12 RBs). The SL-12 RBs that provide an excellent test case of objects that are nominally similar, but may have some unique features or variations amongst the sample. Additionally, we present data on a small set of high area-to-mass ratio (HAMR) and other unusual objects, which will be the subject of a more detailed follow up paper.

2. RAPID PHOTOMETRIC MULTI-COLOR CHARACTERIZATION

Multi-color photometric measurements offer the opportunity to quickly measure the bulk spectral characteristics of a space object. The concept of exploiting the color indices in the visible bands has been previous explored in SSA. For example, BVRI photometry with the Cerro Tololo Inter-American Observatory (CTIO) 0.9 m telescope has been used by Lederer et. al. to compare measured color indices of 18 IDCSP (Initial Defense Communications Satellite Program) satellites with the predictions from laboratory measurements of solar cells [11].

In the asteroid community, Mommert *et. al.* have developed a technique to rapidly characterize newly discovered near Earth asteroids (NEAs) with near-IR photometry [12]. This technique leverages reflectance spectral features in the Z, J, and H bands to distinguish between different classes of asteroids. Instead of spectroscopy, the technique relies on broadband photometry, which results in a more rapid and efficient data collection. This allows asteroids to be characterized quickly during the discovery apparition and before it is lost or too distant to observe. Our technique is a close analog, but applied to the SSA domain. As we have found studying the few published spectra of on-orbit satellites in the near-IR, these same bands are highly diagnostic for satellite characterization, largely due to the strong spectral features typically associated with solar cells in the 1.0-1.1 μm (*c.f.* Figure 2 in [13]) and other strong features in the reflectance spectra of Kapton near 0.5 μm (c.f. Figure 3 in [14]) — both common satellite materials. Consequently, the Z–Y and Z–J color indices are especially diagnostic of solar panel dominated space objects. In the visible part of the spectrum, the Sloan i' (695-844 nm), z_s[1] (826-920 nm), z' (> 820 nm), and Y (950-1058 nm) offer similar diagnostic bands.

[1] Here z_s refers to the specific Astrodon filter which cuts off the open ended Sloan z at 920 nm.

3. FIVE-COLOR NEAR-IR SURVEY

The survey data discussed in this paper were collected with the UKIRT WFCAM between 2 November 2016 and 6 February 2017. Although the details of the collection protocols evolved during the survey, most collections initially acquired the space object near the center of camera 3 in the Z band, then sequenced through the near IR filters Z, Y, J, K, and H. The sequences started with the Z band to maximize detection sensitivity for the initial acquisition. Later protocols shortened the sequence significantly, and finished the sequence with a brief second collection in Z band to provide both astrometric calibration and a photometric reference that could be compared back to the beginning of the track. A typical data collection sequence would take between 10 and 40 minutes.

Figure 1 shows an exemplar sequence of four 5-color data collections on the Galaxy 18 satellite over approximately 2.6 hours. The discontinuities between the different color bands are a visual representation of the color indices that are the subject of our analysis. The slowly decreasing brightness over all color bands during the 2.6 h collection interval is due to the increasing solar phase angle. The light curve shows interesting and dramatic variation in the J band on Galaxy 18, with the Z-Y and Y-J colors dramatically changing with phase angle. In some satellite signatures, a rotational variation is also apparent, but this is often difficult to see in this data as the typical integration times are between 5 and 10 s, and the WFCAM frames are not uniformly spaced. When the satellite rotational variation is comparable to the integration time, this can manifest itself as an apparent random noise in each band, as apparent in the SL-12 RB data collections.

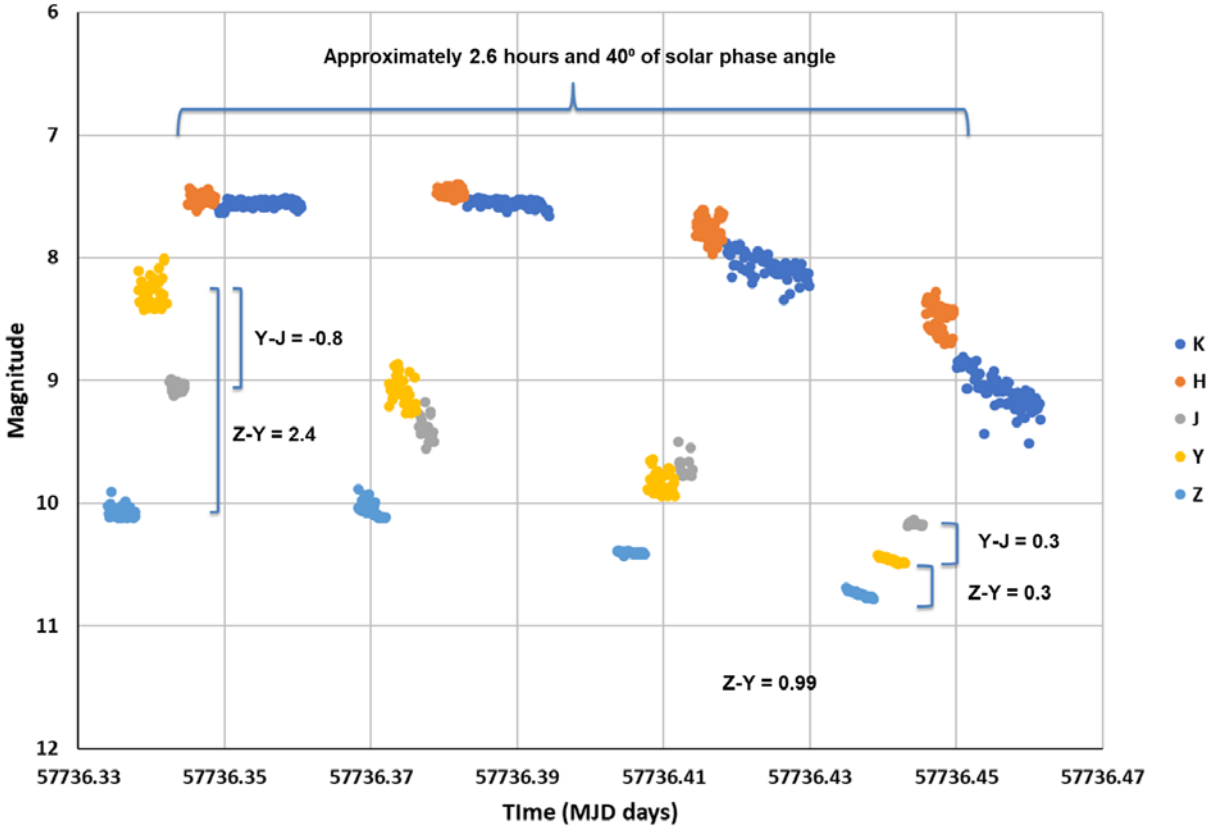

Figure 1. Sequence of 5-color Photometric Collections on Galaxy 18.

4. THE SL-12 ROCKET BODY STUDY

The SL-12 (also called the "Proton K") was a mainstay Russian four-stage to GEO launch vehicle that was used from 1974 to 1994 (see Figure 2) [15, 16]. The SL-12 fourth stage rocket bodies (henceforth referred to as

"SL-12 RB") offer a convenient ensemble of objects for which photometric techniques can be developed and tested. The rocket bodies are bright (11.5 mag in the Z band, or 12 m_v), and at least 25 such objects are available within the longitude range visible from UKIRT to support this study. The SL-12 RB had at least three different versions. The Blok DM (1974) and Blok DM-2 (1982) were similar in structure and fuel, but differed slightly in length. A third version (DM-2M) was developed specifically to support sea launches and is similar structurally to the DM-2. This upper stage was used to insert the payload into GEO from its transfer orbit, and was discarded in GEO without moving it to a graveyard orbit. The SL-12 RB is large, measuring 3.7 m in diameter and approximately 6.2 m long (the DM-2 version). Reportedly the stage could impart a rotation rate of up to 1.5 rpm for spacecraft separation, although observed rotational spin rates of discarded SL-12 rocket bodies are typically significantly faster (5-12 rpm) [17, 18].

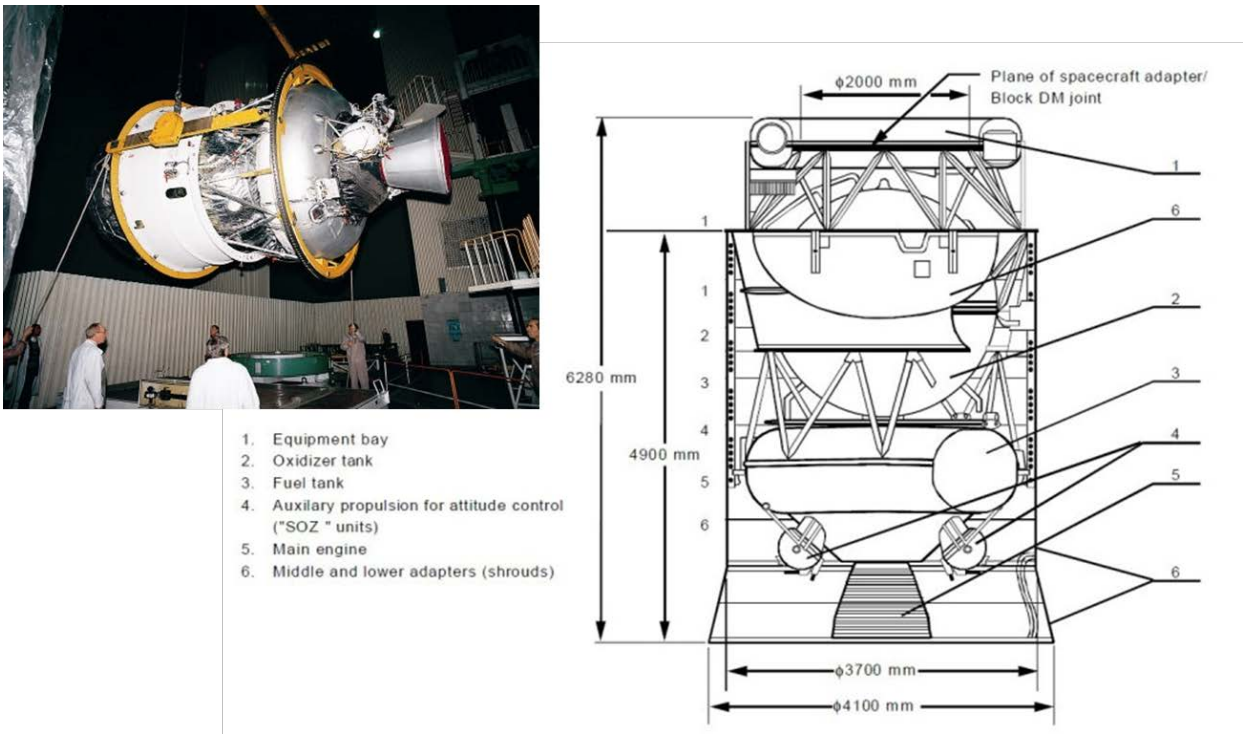

Figure 2. Photograph and Line Drawing of the SL-12 Fourth Stage Rocket Body.

Several authors have published observations and analysis of SL-12 rocket bodies. Researchers at the Kosmoten Station measured several SL-12 RBs and noted that the light curves are "practically identical" [18]. Reflectance spectra 0.65 to 2.5 micron with the NASA Infrared Telescope Facility (IRTF) have been published by Abercromby *et. al.* show the similarities and differences between the SL-12 rocket body and the US Inertia Upper Stages (IUS) [13]. Most relevant to this study, Cardona *et. al*. published an extensive survey of BVRI photometric observations of geosynchronous objects, including 2012-012D and four other SL-12 RBs [19].

This near-IR survey included 55 separate data collections on 24 unique SL-12 RBs that were launched from 1977 to 2012. Examples of both major variants were included in the sample (12 DMs, 12 DM-2s). Figure 3 shows a typical five-color collection on one of the SL-12 RB in our sample, 1987-109D (SCN 18718), an original Blok DM. This collection was our original long ZYJHK observing protocol which cycled through each filter over approximately 39 min. Typical integration times were 5 s in Z, Y, J, and H, and 10 s in K[2]. The longer collection in the K band is a consequence of our early interest in K band for potential thermal emission. Later collections used a quicker 15 min sequence.

[2] Typical sensitivity of WFCAM is 19.1 (Z), 18.7 (Y), 18.1 (J), 17.3 (H), 16.7 (K) in 5 seconds at a SNR of 5.

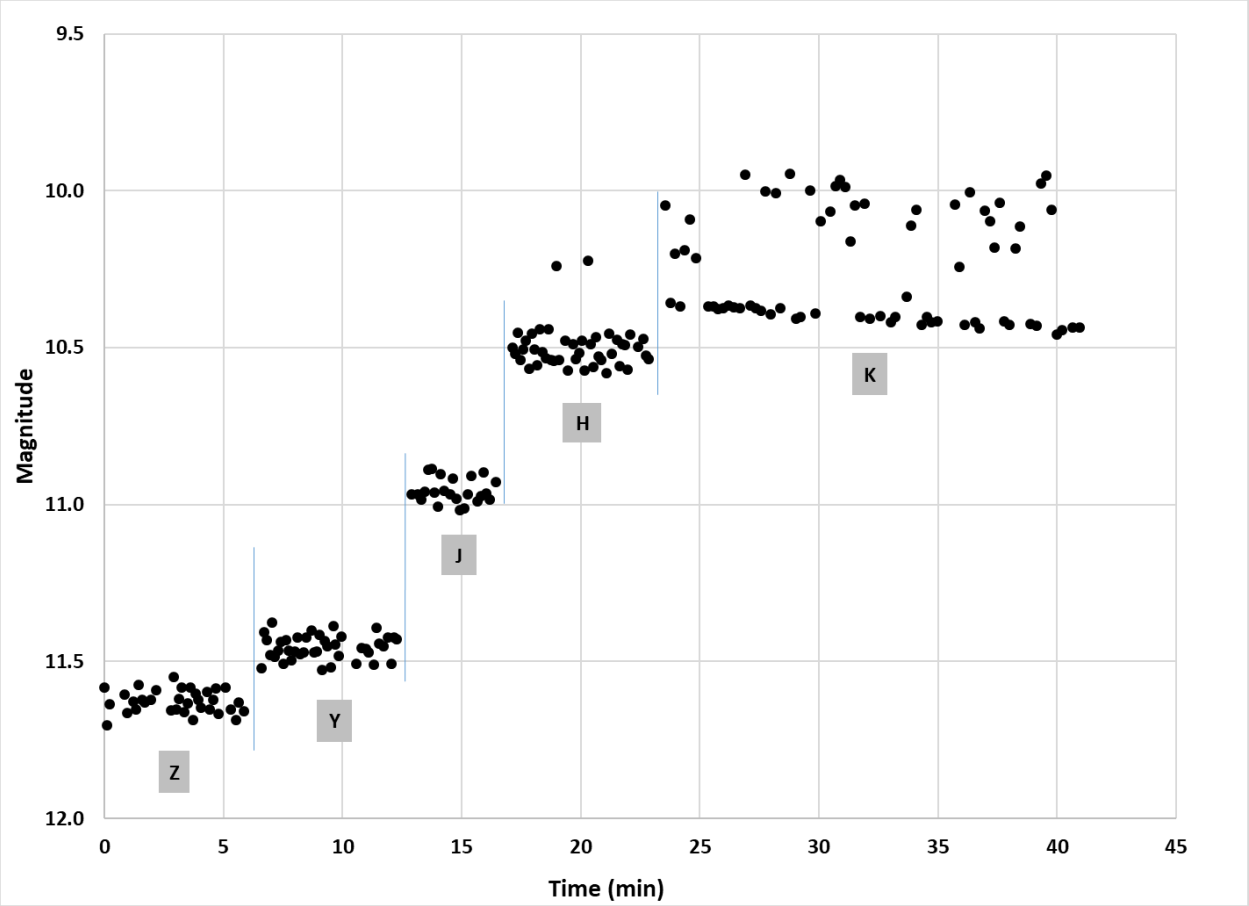

Figure 3. Typical 5-color light curve of an SL-12 RB (1987-109D, SCN 18718).

A visual examination of the light curve reveals the following:

(a) The general downward trend of the light curve is due to the increasing phase angle during the collection (this observation was after opposition).

(b) The discontinuities in the light curve are a manifestation of the color indices. The color indices used for the rapid photometric characterization study where determined by the mean magnitude difference across these gaps. It is these color indices that are the foundation of the rapid photometric characterization techniques being developed.

(c) The apparently random variation in the brightness of 0.1-0.3 magnitudes is due to aliasing of the rotational variation of the SL-12 RB (typically 5-15 s period) with the long integration times with WFCAM (5-10 s), and the somewhat irregular separation between frames inherent in the UKIRT collection.

(d) A common feature of many of the SL-12 RB light curves is the transient brightening in the H and K band. Due to the low time resolution of the UKIRT photometry, further investigation of these features has not been possible with UKIRT. No obvious structure on the SL-12 RB can account for this feature in the light curve, or why it is only observed in the H and K bands.

A visual examination of 45 different light curves of SL-12 RB all show this same general character and when characterized by color indices are tightly clustered as shown in Table 1. However, it became quickly evident that one SL-12 RB was unique. This RB light curve is shown in Figure 4. The overall character of the light curves of 2012-012D and the other SL-12 RBs are somewhat similar. In both examples, the 5-10 s rotational variation is lost in the unevenly spaces 5 s integration time of the UKIRT photometry. However, a closer look at the color indices,

(visually apparent by the discontinuity between the filter changes), shows a significant difference. Most notably, the large Z–J and Y–J colors observed in most SL-12 RB is absent in 2012-012D.

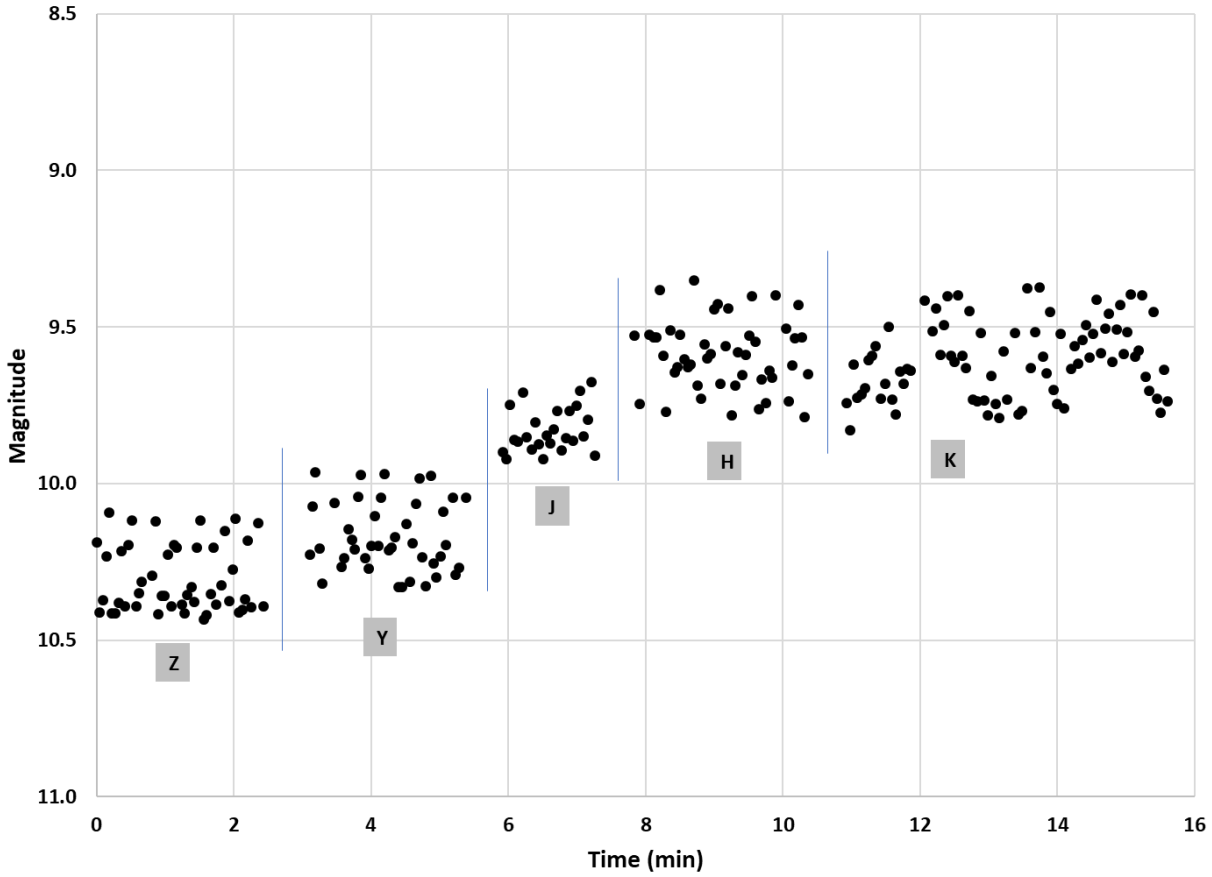

Figure 4. Unusual SL-12 RB 2012-012D (SCN 38104).

Table 1. Color Indices of SL-12 RBs.

	Class	Z-Y	Z-J	Y-J	J-H	H-K	Z-H
Near-IR Colors	not 2012-012D	0.25	0.75	0.50	0.57	0.22	1.33
	2012-012D	0.16	0.49	0.32	0.29	-0.01	0.77
	DM	0.24	0.74	0.51	0.60	0.35	1.37
	DM-2	0.26	0.75	0.50	0.54	0.10	1.30
Solar Relative Near-IR Colors	not 2012-012D ⊙	0.14	0.38	0.25	0.27	0.17	0.66
	2012-012D ⊙	0.05	0.12	0.07	-0.02	-0.06	0.10
	DM ⊙	0.13	0.37	0.25	0.30	0.30	0.69
	DM-2 ⊙	0.15	0.39	0.24	0.24	0.05	0.63

Table 1 details the color indices derived from these light curves for all 24 SL-12 RB measured, including the anomalous 2012-012D. The table lists both the "raw" color indices, as well as the indices expressed relative to the Sun. This allows a direct comparison of the colors to a "grey" satellite. The differences between the unique SL-12 RB 2012-012D and the rest of the population can also be visualized on a color-color diagram as shown in Figure 5. Here the Z–J and Y–J color indices are show in an x-y grid reminiscent of astronomical color-color diagrams used

to study stellar types and evolution. This allows visualization of the clustering of the color indices of the larger class of SL-12 RB and of the unique SL-12 RB 2012-012D. For reference, the Z-J and Y-J color of the Sun is shown by the black dot.

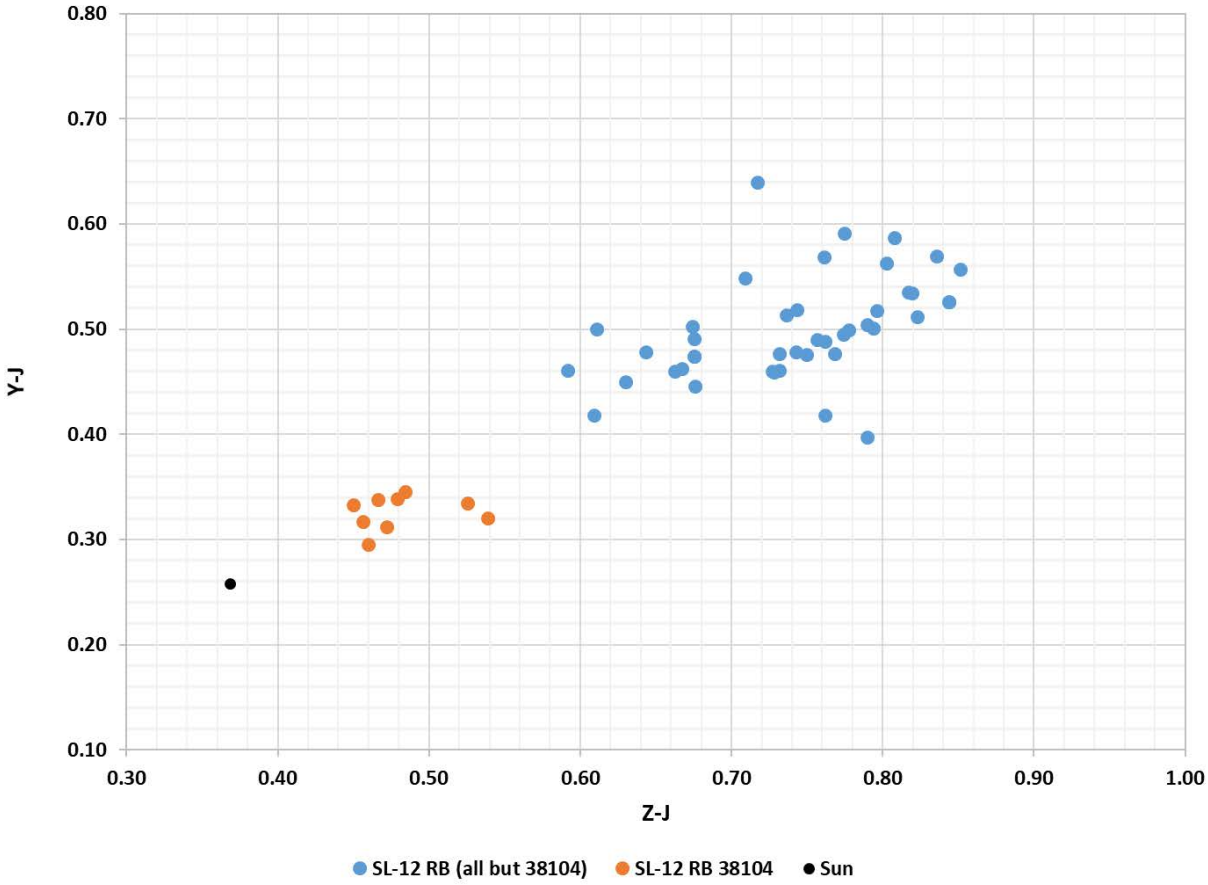

Figure 5. Comparison of Z–J and Y–J color indices of SL-12 RB 2012-012D and all other RBs.

A closer examination of Table 1 shows that the differences between 2012-012D and the rest of the SL-12 RBs is not limited to the Z, Y, and J bands, but extends all the way out to H and K as well. The final color indices, Z–H, spans the entire near-IR range for which reliable data was available for the set of RB as several of the K band measurements were corrupted with the specular reflections features seen in the K band as shown in Figure 3. It is also worth noting that other researchers have published visual colors for SL-12 RBs, including 2012-012D. Specifically, Cardona *et. al.* collected photometric observations of 2012-012D and four other SL-12 RB in 2013 [19]. Although not cited as a finding of their study (Cardona's focus was on-orbit reddening over a wider sample of objects), Cardona's measurements of SL-12 RB color indices suggest that B–V of 2012-012D (B–V 0.39-0.55) is much bluer than the other four SL-12 RBs they measured (B–V of 0.70-0.74).

Because of the discovery of the differences in the near-IR photometric characteristics of 2012-012D, the pedigree and orbital evolution of the RB and its associated payload were investigated. 2012-012D was the upper stage that inserted COSMOS 2479 in March 2012. According to open source, COSMOS 2479 was the eighth and final satellite of the Russian geosynchronous early warning system, US-KMO #8 [21, 22]. It was launched in March 2012, and initially placed at 80 E, and then moved to 166 E by October 2012. In April 2014, it was reported to have failed. This was the last use of the SL-12 for geosynchronous launch by the Russians before retiring the booster. The previous US-KMO launch, which is used here for historical reference, was in June 2008 (COSMOS 2440 and RB 2008-033D, SCN 33111).

In Figure 6 we compare the orbital evolution of the mean motion of the COSMOS 2440 (US-KMO #7) and its RB, to that of COSMOS 2449 and its SL-12 RB 2012-012D for the first 2000 d after arriving at GEO. The

periodic station keeping maneuvers of the payload can be clearly seen, and cease after approximately 500 d as the satellite becomes inactive. The RB, and the payload after it becomes inactive, show the nearly sinusoidal variation in mean motion with no significant secular change in mean motion. This behavior persists to the date of this publication, approximately 3300 d after arrival at GEO.

The lower half of Figure 6 shows the mean motion evolution of the unique SL-12 RB 2012-012 and its payload COSMOS 2479 (US-KMO #8). Again, the station keeping maneuvers of COSMOS 2479 are clearly shown, as well as the maneuver associated with its shift from 80 E to 166 E. The dates of these maneuvers of COSMOS 2479 are consistent with the open source reporting. However, the RB shows a distinctly different behavior of the mean motion than typical inactive objects at GEO. The RB shows a secular increase in the mean motion over the first 1800 d at GEO. The nature of these unusual perturbations has not been determined. These perturbations are especially interesting in the context of the peculiar near-IR and visible color indices.

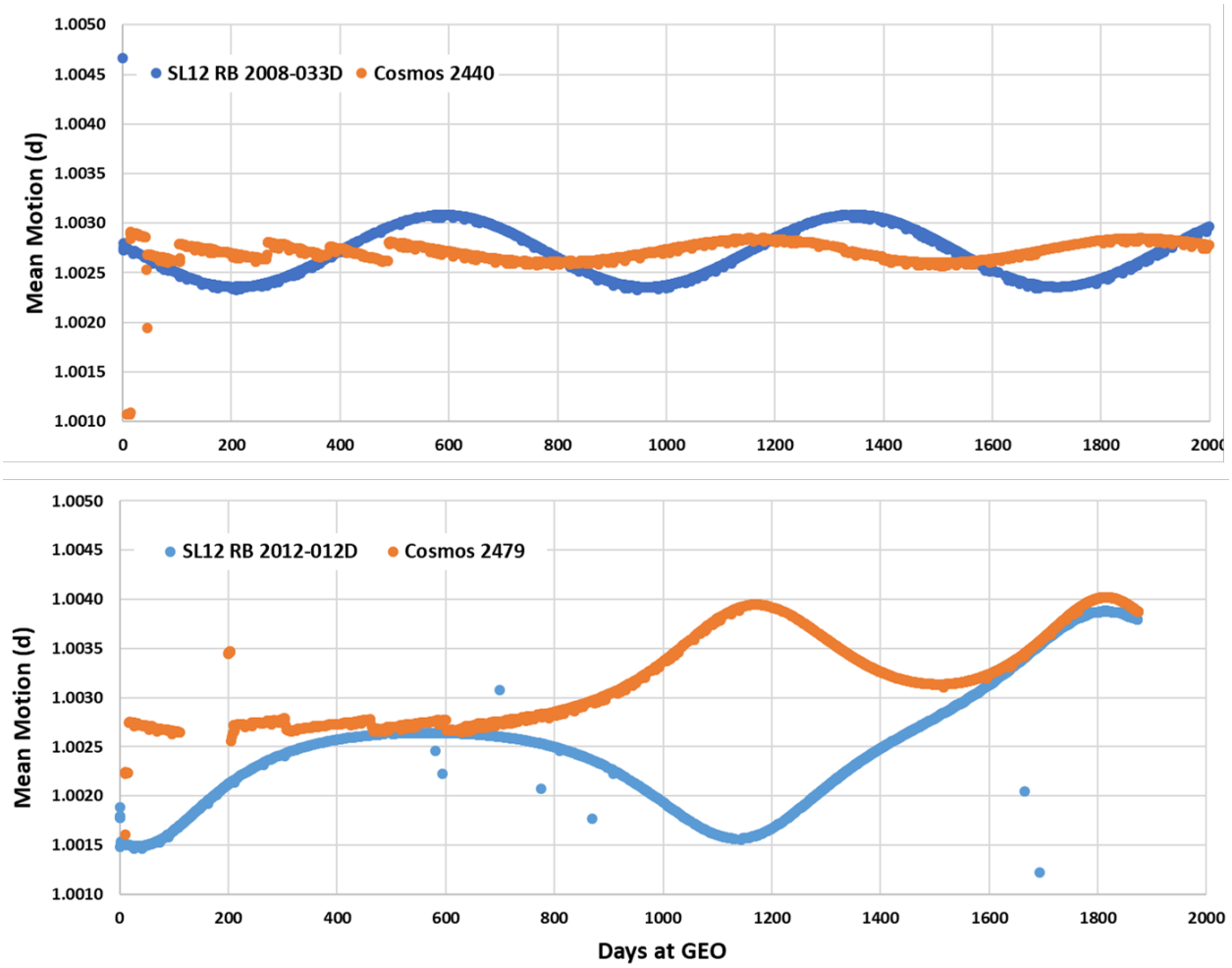

Figure 6. Comparison of the orbital evolution of Cosmos 2479 and RB 2012-012D to the prior launch payload and RB (Cosmos 2440 and 2008-033D).

5. HAMR OBJECT STUDY

The existence of small space objects that have a high enough area-to-mass ratio such that non-gravitational perturbations can dominate their orbital evolution has been a recognized for over twenty years. Such objects were first identified in low Earth orbit space debris surveys by Lincoln Laboratory in 1993 [23]. Later, objects with such characteristics were identified in deep space orbits by the Astronomical Institute University of Bern (AIUB) and the term HAMR (high area-to-mass ratio) object was coined [24]. In deep space, these objects are believed to be debris that has originated from GEO orbit, however, the mechanism of production and material composition remain largely

unknown. Measurements with the ESA 1-m Space Debris Telescope suggest that some HAMR objects may be MLI as indicated by visible band spectroscopy [25]. Due to their small size and large non-gravitational orbital perturbations, HAMR objects are difficult to detect and maintain in a catalog. Consequently, HAMR objects are difficult to study in detail.

As part of this survey, 5-color photometry and light curves were collected on five different HAMR and other unusual objects maintained in a catalog by AIUB/ESA [26]. A summary of the measurements is presented below while a more complete analysis of the HAMR objects studied will be published at a later date. Table 2 summarizes our sample of HAMR objects, which are characterized by a wide range of color indices and light curve behavior that would be expected from debris objects. Perhaps the most unusual object is S95034. Although this object is apparently not in the US catalog, it is in a nearly circular super-synchronous orbit with a very high inclination. As shown in Figure 7, the object is typically bright, with K magnitude of brighter than 10.0, and displays specular flashes as bright as 7.3 in K. The period of this rotation varies greatly, from 700-900 s, and at times will show a significant rotational period change in a single evening. Assuming solar colors, this specular would be approximately 8.6 m_v and its quiescent brightness of approximately 11.3 m_v, suggesting a size of at least 4 m^2.

Table 2. Summary of HAMR Objects Measured.

Object	Epoch	AMR	n	e	i	V	Z
E06321D	57111	2.51	1.0296	0.073	3.2944	15.9±0.7	15.0
E07048A	57111	0.134	0.9246	0.070	21.8788	16.2±0.7	14.6
E16022A	57711	0.0135	1.0464	0.024	0.8162	17.5±1.4	16.8
S95034	57711	0.0143	0.9432	0.002	16.4823	12.3±1.2	11.9
S95105	57770	0.0088	0.9969	0.134	6.8950	13.0±0.6	11.2

Object	Z	Z-Y	Z-J	Y-J	J-H	K-H	p	
E06321D	15.0	0.02	0.40	0.38	0.28	0.07	21 s	Very large 1-2 mag rotational variation
E07048A	14.6	0.24	0.64	0.40	0.35	-0.40	120-180 s	J and H excess, K-H most extreme of all objects surveyed, complex tumble
E16022A	16.8	0.12	0.44	0.32	0.07	N/A	none	Faint, solar panel like Z-J
S95034	11.9	0.33	0.85	0.77	0.21	0.15	700-900 s	Extremely bright specular, variable period
S95105	11.2	0.32	0.90	0.58	0.61	0.25	none	No obvious period, high Z-Y

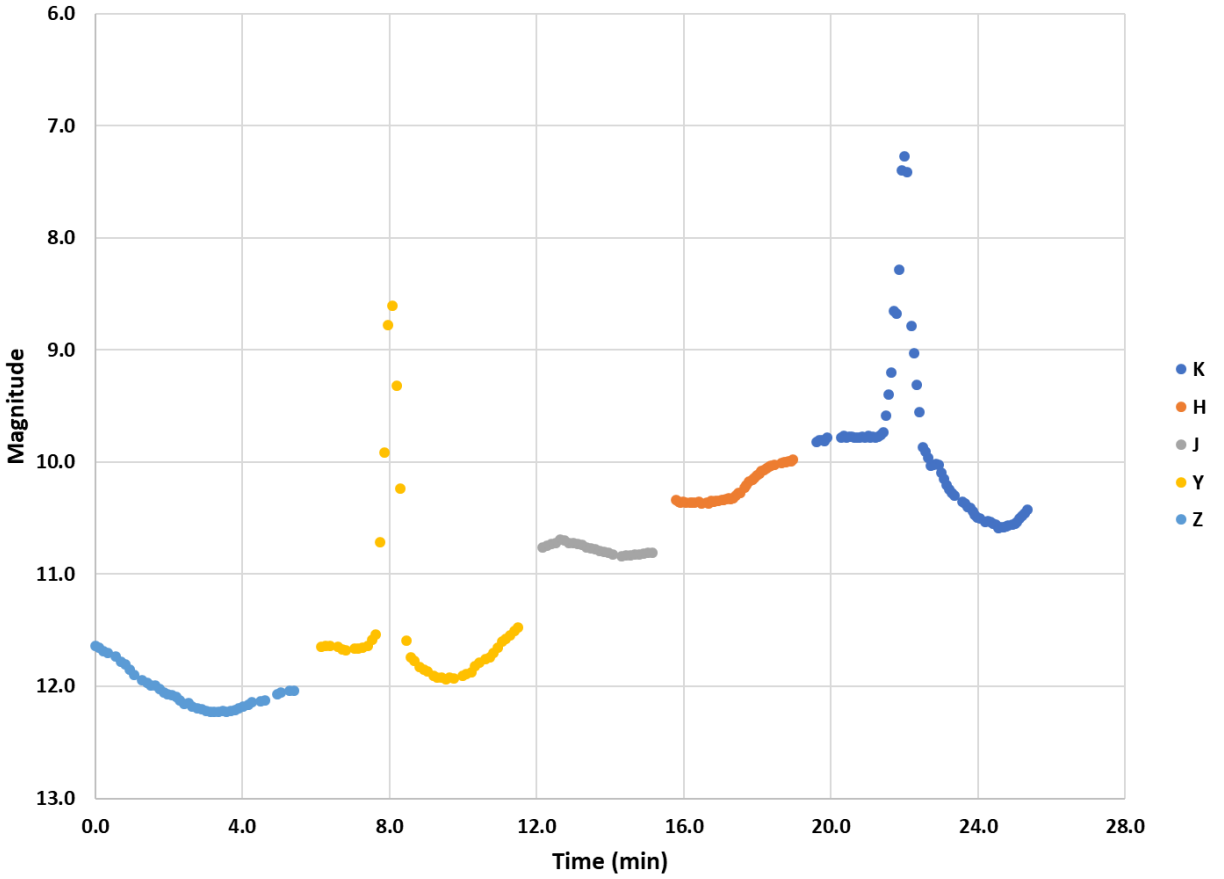

Figure 7. Five-Color Collection of HAMR Object S95034 showing bright specular flashes.

6. CONCLUSION

We have completed the first phase of a comprehensive 5-color near-IR survey with the UKIRT telescope and WFCAM instrument. In our initial analysis, the efficacy of rapid characterization of space objects with techniques similar to that used by the astronomical community with near Earth asteroids has been demonstrated. Using a sample of SL-12 RB, one object was identified (2012-012D) as an exemplar of an object recognized definitively as anomalous in its class and discovered to be experiencing unusual secular orbital perturbations. We have also surveyed several HAMR and other unusual objects that are not currently maintained in the US catalog.

Based on the lessons of the first UKIRT measurements, we are refining our observing protocol to more quickly and unambiguously extract color indices and minimize confusion by phase angle or rotational changes during the collection. With UKIRT WFCAM this must forge a compromise minimizing filter changes, collecting adequate data in each band to average out rotational variation, and complete the collection quickly enough to be robust to phase angle and weather changes. The ideal situation would be to simultaneously collect in each band. These concepts are being incorporated into a high-speed three channel photometer “Chimera” for SSA applications in a related University of Arizona program. Chimera will collect simultaneous three-color photometry in the Sloan r’, i’, and z’ bands at rates exceeding 1 kHz using three commercially available EM-CCD cameras. After initial demonstration of Chimera, we hope to extend the instrument with two additional near-IR channels.

We anticipate that the techniques will also prove themselves over a broader class of objects, especially since the near-IR bands are particularly diagnostic of the spectral features surrounding the solar panel band gap feature. This will allow quick discrimination between space debris and solar-panel covered microsatellites that would otherwise be of similar brightness.

7. ACKNOWLEDGEMENTS

This work was funded by the University of Arizona Office of Research, Discovery and Innovation.

Operational and scientific support for UKIRT observations of orbital debris was provided by the Lockheed Martin Advanced Technology Center under a contract with NASA.

Historical two-line element sets for this analysis were provided by CelesTrak (https://celestrak.com/).

8. REFERENCES

1. J. G. Moore, "Photometric Observations of the Second Soviet Satellite (1957 β1)," *Publications of the Astronomical Society of the Pacific*, vol. 71, (419), pp. 163-165, 1959.
2. V. M. Grigorevskij, "About Methods of Photometry of Artificial Earth's Satellites," Byulleten' Stantsii Nablyudenia ISZ, No. 7, p. 14, 1959.
3. J. V. Lambert and K.E. Kissell, "The Early Development of Satellite Characterization Capabilities at the Air Force Laboratories," in *Proceedings of the Advanced Maui Optical and Space Surveillance Technologies (AMOS) Conference*, Wailea, Maui, Hawaii, 2006.
4. P. P. Sukhov and K. P. Sukhov, "On some problems of photometric identification of geostationary satellites," Kinematics and Physics of Celestial Bodies, vol. 31, (6), pp. 314-318, 2015.
5. J. M. Souvari, "Photometry of Artificial Satellites Application to the Ground Electro-Optical Deep Space Surveillance (GEODSS) Program," *MIT Lincoln Laboratory Technical Note 1979-61*, 1979.
6. T. E. Payne *et al*, "Color Photometry of Geosynchronous Satellites Using the SILC Filters", *Proceedings of SPIE*, vol. 4490/no. 1, pp. 194-199, 2001.
7. T. E. Payne *et al*, "Analysis of Multispectral Radiometric Signatures from Geosynchronous Satellites," *Proceedings of SPIE*, vol. 4847/no. 1, pp. 332-336., 2002.
8. T. Schildknecht *et al*, "Color Photometry and Light Curve Observations of Space Debris in GEO," in *Proceedings of the Advanced Maui Optical and Space Surveillance Technologies (AMOS) Conference*, Wailea, Maui, Hawaii, 2008.
9. R. Kendrick *et al*, "GEO Belt Survey with WFCAM," in *Proceedings of the Advanced Maui Optical and Space Surveillance Technologies (AMOS) Conference*, Wailea, Maui, Hawaii, 2014.
10. M. Casali *et al*, "The UKIRT Wide-field Camera," *Astronomy and Astrophysics*, vol. 467, (2), pp. 777-784, 2007.
11. S.M. Lederer *et al*, "Preliminary Characterization of IDCSP Spacecrafts through a Multi-Analytical Approach," in *Proceedings of the Advanced Maui Optical and Space Surveillance Technologies (AMOS) Conference*, Wailea, Maui, Hawaii, 2012.
12. M. Mommert *et al*, "First Results from the Rapid-response Spectrophotometric Characterization of Near-Earth Objects using UKIRT", *Astronomical Journal*, vol. 151, (4), 2016.
13. K. J. Abercromby, P. Abell, and E. Baker, "Reflectance Spectra Comparison of Orbital Debris, Intact Spacecraft, and Intact Rocket Bodies in the GEO regime," *Fifth European Conference on Space Debris*, Darmstadt, Germany, 2009.
14. L. Bai *et al*, "Spectral scattering characteristics of space target in near-UV to visible bands," *Optical Express* vol. 22, (7), pp. 8515-8524, 2014.
15. Gunter's Space Page, "Blok-D," available: http://space.skyrocket.de/doc_stage/blok-d.htm, 2017.
16. CAPCOM ESPACE, "The Launchers D (US 500 SL-12/13)," available: https://www.capcomespace.net/dossiers/espace_sovietique/lanceurs/lanceurs_D.htm 2017.
17. "Mission Overview GE-6 Launch on the Proton Launch Vehicle," International Launch Services, 2000.

18. V. S. Yurasov, V. G. Vygon, and V.D. Shargorodskiy, "Classification and Identification of Geostationary Space Objects by Using Coordinate and Photometric Observations," in *Proceedings of the Sixth US/Russian Space Surveillance Workshop*, Russian Academy of Science, St. Petersburg, Russia, 2005.

19. T. Cardona, *et al*, "BVRI Photometric Observations and Light-Curve Analysis of GEO Objects," *Advances in Space Research*, vol. 58, pp. 514-527, 2016.

20. F. Santoni, E. Cordelli, and F. Piergentili, "Rocket Body Rotational State Estimation by Remote Optical Observations", in *Proceedings of the International Astronautical Congress*, IAC, vol. 4, pp. 2711-2719, 2012.

21. Russian Strategic Nuclear Forces, "Changes in Russia's Early Warning Satellite Constellation," available: http://russianforces.org/blog/2012/11/changes_in_russias_early_warni.shtml, 2012. 13 November.

22. A. Paleologue, "Early Warning Satellites in Russia: What past, what state today, what future?", Proceedings SPIE, vol. 5799, (1), pp. 146-157, 2005.

23. E. C. Pearce, M. S. Blythe, D. M. Gibson, P. J. Trujillo, "Space Debris Measurements: Phase One Final Report," in *Proceedings of the 1994 Space Surveillance Workshop*, MIT Lincoln Laboratory Project Report STK-221, vol. 1, p.125, 1994.

24. T. Schildknecht *et al*. "Optical Observations of Space Debris in GEO and in Highly Eccentric Orbits", *Advances in Space Research*, vol. 34, pp. 901-911, 2004.

25. A. Vananti, T. Schildknecht and H. Krag, "Reflectance Spectroscopy Characterization of Space Debris," *Advances in Space Research*, vol. 59, (10), pp. 2488-2500, 2017;2016

26. C. Fruh, and T. Schildknecht, "Variation of the Area-to-mass Ratio of High Area-to-mass Ratio Space Debris Objects", *Monthly Notices of the Royal Astronomical Society*, vol. 419, (4), pp. 3521-3528, 2012.